processes

MDPI

Article

Process Simulation and Optimization of Fluid Catalytic Cracking Unit's Rich Gas Compression System and Absorption Stabilization System

Jin Sun [1], Haoshui Yu [2,*], Zengqi Yin [3], Liangliang Jiang [4], Li Wang [1], Shaolin Hu [1] and Rujin Zhou [1,*]

[1] School of Chemical Engineering, Guangdong University of Petrochemical Technology, Maoming 525000, China; sunjin@gdupt.edu.cn (J.S.); hfkth@gdupt.edu.cn (S.H.)
[2] Department of Chemistry and Bioscience, Aalborg University, 6700 Esbjerg, Denmark
[3] China Petroleum & Chemical Corporation Maoming Branch, Maoming 525000, China; yinzq6038.mmsh@sinopec.com
[4] Chemical and Petroleum Department, University of Calgary, Calgary, AB T2N 1N4, Canada; jial@ucalgary.ca
* Correspondence: hayu@bio.aau.dk (H.Y.); rujinzhou@gdupt.edu.cn (R.Z.); Tel.: +86-668-2858690 (R.Z.)

Abstract: In a fuel-based refinery, rich gas in the fluid catalytic cracking (FCC) unit is further processed to separate dry gas and refinery products (i.e., stabilized gasoline and liquified petroleum gas). The process is utility-intensive and costly and includes a two-stage compressor, pumps, an absorber, a stripper, a stabilizer, and a re-absorber. The optimization was conducted with respect to the compressor outlet pressure from the gas compression system (GCS) and the flow rate of absorbent and supplementary absorbent from the Absorption-stabilization System (ASS) using the process simulation software Aspen Plus. Compared to the base case of a 725 kt/a rich gas FCC unit, a refinery can save 2.42% of utility costs under optimal operation. Through optimized operation, medium-pressure steam consumption has been reduced by 2.4% compared to the base case, resulting in a significant improvement in total operational cost. The optimization strategy can provide insightful guidance for the practical operation of GCS and ASS.

Keywords: fuel-based refinery; rich gas; fluid catalytic cracking; Aspen Plus; absorption-stabilization system

check for updates

Citation: Sun, J.; Yu, H.; Yin, Z.; Jiang, L.; Wang, L.; Hu, S.; Zhou, R. Process Simulation and Optimization of Fluid Catalytic Cracking Unit's Rich Gas Compression System and Absorption Stabilization System. *Processes* **2023**, *11*, 2140. https://doi.org/10.3390/pr11072140

Academic Editor: Gade Pandu Rangaiah

Received: 6 June 2023
Revised: 11 July 2023
Accepted: 14 July 2023
Published: 18 July 2023

Copyright: © 2023 by the authors. Licensee MDPI, Basel, Switzerland. This article is an open access article distributed under the terms and conditions of the Creative Commons Attribution (CC BY) license (https://creativecommons.org/licenses/by/4.0/).

1. Introduction

Currently, crude oils are getting scarcer and more expensive, and the need for light oil is continually rising. Oil deep processing, especially under cost-effective energy management, is essential. The FCC unit is a significant deep processing procedure for crude oil, a high-energy-consuming component of a fuel-based refinery, and is undergoing extraordinary development [1]. The FCC is the modern refinery's mainstay on a global scale. Its purpose was to transform heavy hydrocarbon petroleum compounds into a variety of more usable products, including petrol, intermediate distillates, and light olefins [2]. The product from the FCC reaction is then separated into rich gas, unsaturated gasoline, light diesel oil, re-refined oil, and oil slurry based on the various boiling point ranges of the distillates, while also making sure that the dry point, freezing point, and flash point of light diesel oil are acceptable [3]. Compressed-rich gas (H_2, CO, CO_2, $C_{1–6}$ components) and crude gasoline are distillated from the top of the main fractionation tower are commonly co-processed in ASS. Prior to ASS, a two-stage turbine was used to compress the rich gas to the required pressure for the subsequent operation. In particular, the dry gas ($C_{2–}$ components) and liquefied petroleum gas (LPG, $C_{3–4}$ components) are separated from the compressed rich gas, while the stabilized gasoline is upgraded from crude gasoline in this process [4]. The ASS comprises four columns: absorber, desorber, reabsorber, and stabilizer [5,6]. As the ASS consists of four recycles with substantial flow rates, the interaction between the various

process parameters is intense. As an illustration, the absorber and desorber interact closely because they feed each other. Specifically, the rich absorption oil from the absorption tower is the liquid feed for the desorption tower. Likewise, the desorbed gas from the desorption tower is recycled as the gas feed to the absorption tower, as shown in Figure 1. The system's temperature and pressure influence the absorption and desorption effects. There is a tradeoff between desorbed gas quantity, dry gas quality, and LPG quality [7]. Chen et al. [8] introduced a novel GASP to enhance the separation process and greatly simplify the existing GASP flowsheet. They analyzed the solubility and volatility of the C_5–C_{11} hydrocarbons in their study and introduced a new indicator to reflect the effectiveness of additional absorbent streams. Pan et al. [9] presented a rigorous dynamic simulation of the fluid catalytic cracking unit's (FCCU) absorption-stabilization system.

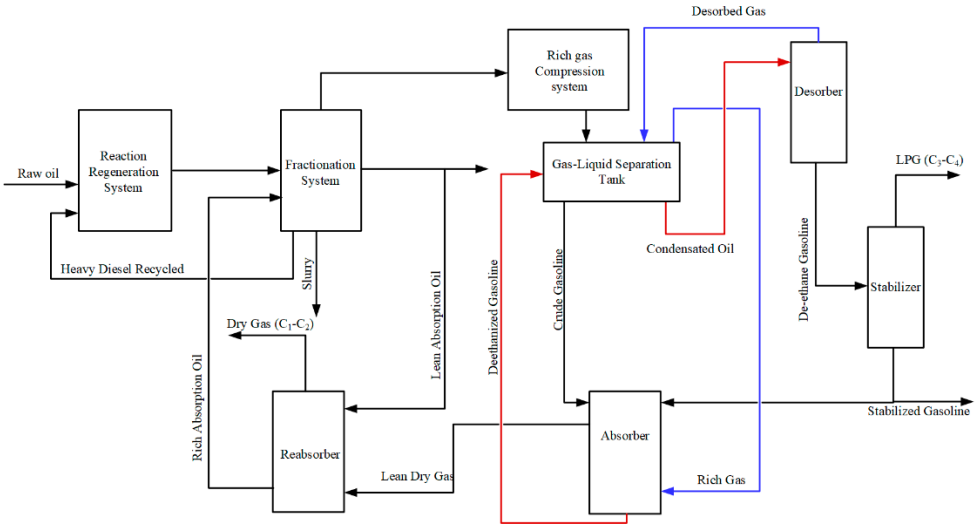


Figure 1. The FCC process diagram including reaction-regeneration, fractionation, compression, and absorption-stabilization processes.

The issues with the GCS and ASS have been investigated by other researchers in terms of process modeling, simulation, and operational optimization. Liu et al. [10] used process simulation and pinch analysis to conduct a thorough investigation of the process retrofit along with heat integration for an existing ASS with feed splitting. They introduced a new ASS with a two-stage condensation section. Zhang et al. [11] employed HYSYS software to model the mechanism of the FCC unit and proposed an optimization method to improve the product yield and processing capacity through the model research. Liu et al. [12] simulated the FCC flowsheet and proposed case studies to quantify the effects of key FCC operating variables. Sui et al. [13] employed an organic rankine cycle (ORC) to convert low-grade process heat to electricity by integrating it into the fluid catalytic cracking (FCC) absorption-stabilization system. Yang et al. [14] have proposed a brand-new flowsheet that uses less energy by adding a side extraction stream to the absorber. Pinheiro et al. [15] explored novel developments in the modeling, monitoring, control, and optimization of the fluid catalytic cracking (FCC) process. He et al. [16] proposed a modeling strategy that combines molecular mechanisms and data models to explain the maximizing iso-paraffins (MIP) technology of the FCC process.

Therefore, much research is required to gain a thorough grasp of the two systems. Only in this manner can an optimal design be achieved. The impact of the GCS outlet pressure on the ASS absorption efficiency, however, was not taken into account by the aforementioned literature as a crucial decision variable to be optimized. Given the above literature, we can suggest that changing the outlet pressure of GCS and the inlet flowrate of absorbent to the absorption tower in ASS would effectively intensify the mass transfer and absorption efficiency of the absorber and further improve the utility-use performance of the existing GCS and ASS.

The flow rate and inlet temperature of unsaturated gasoline and diesel from the main fractionator and the supplementary absorbent from the stabilizer plays a vital role in the absorption efficiency of absorbers, reducing C_{3+} light components in lean gas and dry gas from the top of the absorber and reabsorber, respectively. The operational pressure, flow rate, and temperature of the absorbent are key parameters to the absorption process. Higher pressure and flow rate and lower inlet temperature of the absorbent are beneficial for absorption. The absorbent temperature cannot be reduced below 40 °C due to the limitations of the temperature of fresh cooling water. Thus, the energy-saving effects are relatively limited by optimizing the inlet temperature of the absorbent. However, the electricity consumption of rich gas compressors and pumps will be increased correspondingly along with the increment of the outlet pressure of the compressor, tower pressure of absorber, and quantity of the absorbents. Hence, there is a tradeoff between the compression system and absorption-stabilization system. In the past, few researchers optimized these two key parameters simultaneously.

The objective of this paper is to conduct a systematic study on process retrofit through process simulation and optimization on the upstream GCS and downstream ASS. The key novelty of this work is the simultaneous consideration of tower operational pressure and absorbent flow rate for the energy-use efficiency of the two systems mentioned above.

2. Process Description of GCS and ASS

2.1. Rich Gas Compression System

Note that the specifications are all derived from industrial data. The primary fractionator is responsible for separating wet gases, naphtha, light gas oil, heavy cycle oil, and slurry oil from high-temperature superheated reaction vapor from the catalytic reactor. Separate wet gases and naphtha into dry gas, liquefied petroleum gas (LPG), and gasoline using the GCS and the ASS. The rich gas compressor's duty is to increase the rich gas's pressure from the fractionation process to the pressure required for the ASS to operate. The main factors affecting the energy consumption of the rich gas compressor are gas flow rate, compression ratio, and the selection of driving power. Compared with a single-stage compressor, a two-stage compressor can save 15 kWh per ton of rich gas. The back-pressure steam turbine has the lowest overall energy usage. The energy consumption ratio of the condensing steam turbine, electric motor, and back-pressure steam turbine under the same compression load is around 0.62:0.33:0.12 [17]. The rich gas compressor is driven by the back-pressure compressor using medium-pressure steam (around 3.5 MPa). The reboiler of the stabilization tower and desorption tower in ASS can be heated using the low-pressure steam (around 1 MPa) emitted from the compressor outlet.

A two-stage centrifugal compressor is utilized in the wet gas compressor. Typically, this type of compressor uses an electric motor driven by high-pressure steam or a multistage turbine. The steam is frequently vented to a surface condenser operating in a vacuum. In two-stage systems, the vapors from the compressor's first-stage discharge are often partially condensed and flashed in an inter-stage drum. In the gas plant, the liquid hydrocarbon is pumped either to the high-pressure separator (HPS) or right to the stripper. GCS consists of a two-stage compressor. The detailed compression process is as follows: The rich gas (S1), separated from the main fractionator, enters a first-stage compressor (C1) for compression. Then it is cooled by cooling water to 40 °C for vapor-liquid separation in an interstage flash (D1). The rich compressed gas enters the second-stage compressor (C2) for further compression. Then it is wasted with acid water (S47) and cooled by the dry air cooler (E1), as shown in Figure 2.

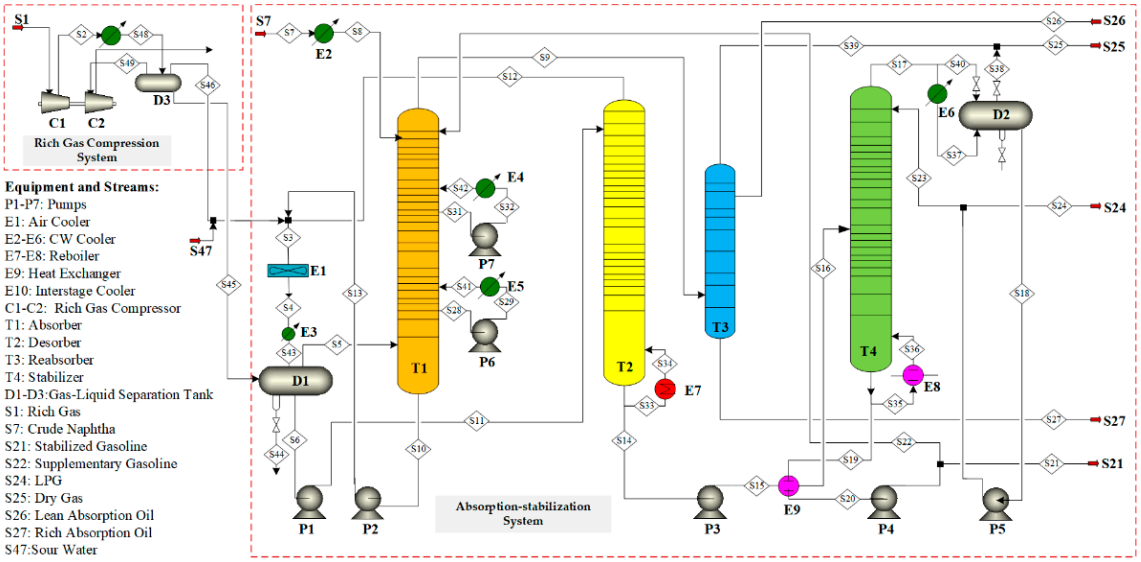


Figure 2. The flowsheet of the rich gas compression system and absorption-stabilization system in the existing FCC unit.

2.2. Absorption-Stabilization System

The absorber, desorber, reabsorber, and stabilizer constitute the majority of the ASS, together with corresponding heat exchangers and other auxiliary equipment. The primary goal of the system is to separate the rich gas and unsaturated gasoline produced by the main fractionator into dry gas (C_1–C_2), LPG (C_3–C_4), and stabilized gasoline with a suitable vapor pressure.

The detailed ASS is as follows: mixing the compressed rich gas (S47), the absorber bottom oil (S13), and the desorbed gas from the desorber (S12) for gas-liquid balancing in a gas-liquid balance tank (D1), and introducing the condensate oil (S11) at the bottom of the tank into the desorber (T2); the top of the absorber (T1) discharges lean dry gas (S9), and the gas passes through the de-ethanized gasoline (S14) and enters the stabilizer (T4), which evaporates light components lighter than C_4 from the de-ethanized gasoline, and LPG (S24) primarily containing C_3 and C_4 is obtained at the top of the stabilizer. The bottom product is the stabilized gasoline (S21) with the qualified vapor pressure and is cooled to 40 °C. A portion of the stabilized gasoline returns to the top of the absorber to serve as a supplementary absorbent (S22), and the rest of the bottom product is discharged from the pump (P4) as products. To increase the absorption efficiency of the absorber, it is typically equipped with intermediate coolers (E4 and E5) for heat extraction in the middle of the tower to ensure low-temperature absorption.

3. Simulation and Optimization of Existing GCS and ASS

3.1. Case Study One

We take a 725 kt/a rich gas processing flowsheet of an FCC refinery in China as the research object. Figure 3 illustrates the overall Aspen Plus model of GCS and ASS. In this work, the Aspen Plus V12.0 simulator is used to represent this integrated system. For predicting the thermodynamic properties of all fluids, the Peng–Robinson state equation is chosen. Table A1 lists Data of streams on the rich gas compression system and absorption stabilization system in Appendix A. The optimization module is utilized for optimization purposes.

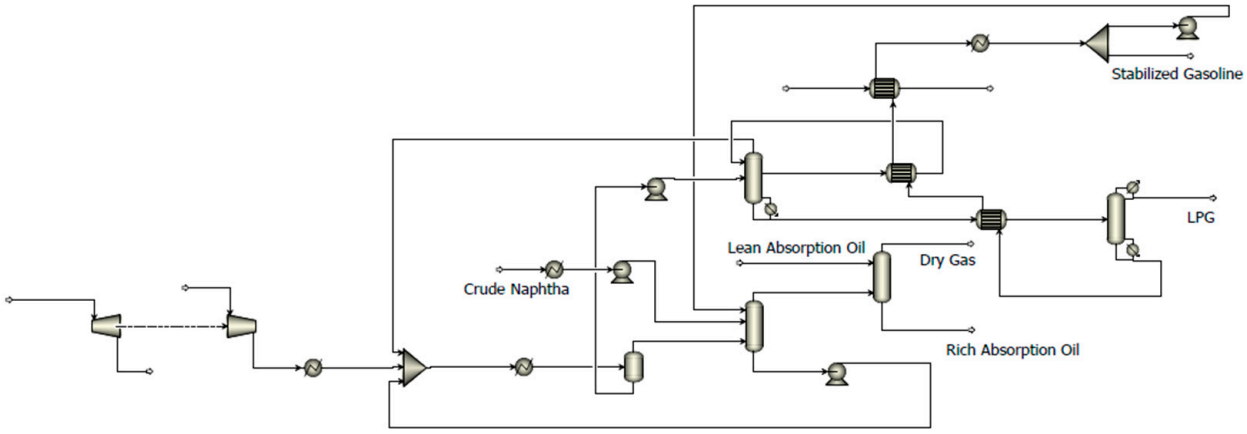


Figure 3. Simulation of FCC absorption-stabilization system including rich gas compression.

A "RadFrac" module is used to simulate each of the four distillation columns. In this study, there are five recycle streams in the ASS: two pumparounds as coolers for absorber, intermediate heater recycle for desorber, recycled desorbed gas, rich absorption oil, and supplemental absorbent. To avoid the convergence issue, we divide the recycle streams in the simulation model and connect them until the difference between the values of the divided streams becomes negligible. This simulation technique has been extensively studied in the literature [18].

Tables 1 and 2 list the property parameters of all feed streams (S1, S7, S27 in Figure 2) including molar percentage (mol%), pressure (P), temperature (T), mass flow rate (F), density (ρ, tested at 20 °C), and the true boiling point (TBP).

Table 1. Components of the Rich Gas for stream S1 in the existing GCS.

Components	Alias	Molar Fraction Composition (%)
Hydrogen	H_2	7.61
Water	H_2O	0
Nitrogen	N_2	10.51
Oxygen	O_2	1.23
Carbon-monoxide	CO	0.71
Carbon-dioxide	CO_2	1.24
Methane	CH_4	11.12
Ethylene	C_2H_4	5.26
Ethane	C_2H_6	5.91
Propylene	C_3H_6-2	14.65
Propane	C_3H_8	7.86
1,3-Butadiene	C_4H_6-4	0.05
1-Butene	C_4H_8-1	3.47
Cis-2-Butene	C_4H_8-2	2.35
Trans-2-Butene	C_4H_8-3	1.82
Iso-Butene	C_4H_8-5	2.09
N-Butane	C_4H_{10}-1	3.55
Iso-Butane	C_4H_{10}-2	8.98
N-Pentane	C_5H_{12}-1	0.72
2-Methyl-Butane	C_5H_{12}-2	5.62
N-Hexane	C_6H_{14}-1	5.25

Table 2. Parameters of absorbents for stream S7 and S26 in existing ASS.

Stream	P/MPa	T/°C	F/(kg·h)	ρ/(kg·m^3)	The TBP Distillation Curve (%)						
					IBP *	10	30	50	70	90	EBP *
Crude naphtha	1.2	30	48,998	735.7	53	93	115	135	154	180	204
lean absorption oil	1.2	35	79,974	827.2	188	226	249	272	303	332	342

* IBP and EBP signify the initial boiling point and end boiling point, respectively.

The specifications of the absorber, desorber, stabilizer, reabsorber, and compressor are listed in Table 3. Thus, to guarantee the LPG quality, this model specifies that the concentrations of the total $C_{1–2}$ components in the desorbed oil should be lower than 7.0 mol%. Here, RVP is Reid Vapor Pressure, which represents gasoline vapor pressure with a quarter volumetric ratio of vapor to oil at 37.8 °C. The molar concentrations of the total $C_{1–4}$ components at the bottom stream of the stabilized tower are specified to be less than 1.0 mol% to meet the product specifications of the stabilized gasoline.

Table 3. Specifications of the absorber, desorber, stabilizer, reabsorber, stabilizer, and compressor.

Devices	P/MPa	No. of Stage	Feed Stage	Specifications		Variables
				Distillate	Bottom	
Absober	1.24	20	1/2/20	$C_{3–4} \leq 2$ mol%	NA	S22 * flow rate in T1
Desorber	1.5	20	1/10 *	NA	$C_{1–2} \leq 0.7$ mol%	E7 Reboiler duty in T2
Reabsorber	1.13	7	1/7	$C_{3–6} \leq 3$ mol%	NA	S26 * flow rate in T3
Stabilizer	1.2	20	10	$C_{1–2} \leq 3$ mol%, $C_{5–6} \leq 1.5$ mol%	$C_{3–4} \leq 1$ mol%, RVP $\leq$ 65 kPa	Reflux ratio in T4 E8 Reboiler duty in T4
Compressor outlet	≥1.26	-	-	-	-	3.5 MPa steam flow rate for turbine

* 10, S22, S26 signify pumparound feed stage, supplementary gasoline, and lean absorption oil in Figure 2.

Olefins in the rich gas, especially propylene, are valuable chemical raw materials. The LPG in the ASS should contain as much propylene as possible, and the amount of propylene and butene entrained in the dry gas should be limited as much as possible. Specifically, $C_{3–6}$ molar concentrations of the dry gas product in S25 should be lower than 3 mol%. The light diesel oil is used only to absorb C_{5+} components in the reabsorption tower.

Table 4 compares simulation results with industrial data, indicating a high level of agreement. It also demonstrates that the thermodynamic method of Peng-Robinson and the simulation strategy utilized in this model are capable of producing accurate and reliable simulations.

Table 4. Comparison of operation parameters for the existing system.

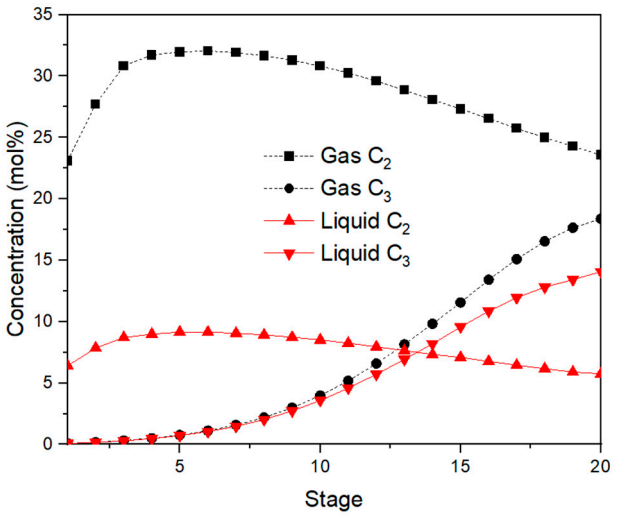
Item	Simulation Parameters	Unit	Industrial Values	Simulated Values
Feed Streams	Compressed rich gas	t/h	86.417	85.107
	Crude gasoline	t/h	49.142	48.856
	Lean absorption oil	t/h	18.118	17.449
	Subtotal	t/h	153.677	151.412
Product streams	Dry gas	t/h	19.128	19.117
	Liquefied petroleum gas	t/h	49.395	48.515
	Stabilized gasoline	t/h	65.136	64.063
	Rich absorption oil	t/h	18.154	19.717
	Subtotal	t/h	151.813	151.412

Table 4. *Cont.*

Item	Simulation Parameters	Unit	Industrial Values	Simulated Values
Loss	Discharge or leakage loss	t/h	1.864	0
Absorber	Top temperature	°C	33.7	33.8
	Bottom temperature	°C	45.6	45.4
	Top pressure	MPa	1.24	1.24
Reabsorber	Top temperature	°C	38.4	38.2
	Bottom temperature	°C	43.3	42.5
	Top pressure	MPa	1.18	1.13
Desorber	Top temperature	°C	44.3	45
	Bottom temperature	°C	56.3	54.4
	Top pressure	MPa	1.53	1.52
Stabilizer	Top temperature	°C	47.5	47.3
	Bottom temperature	°C	187.4	190.6
	Top pressure	MPa	1.13	1.2

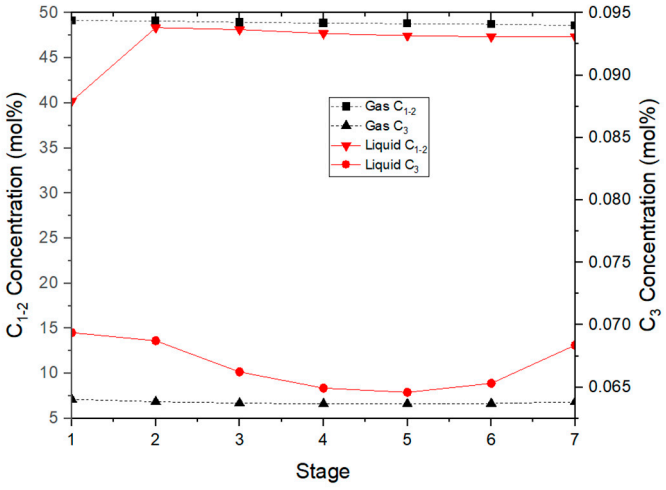
3.2. Gas-Liquid Concentration Distribution Analysis of the Towers

Both the absorption and reabsorption towers are used to absorb C_{3+} components from compressed rich gas and recover C_{2-} components (i.e., dry gas). Additionally, the stabilization tower is used to simultaneously separate C_{4-} (LPG) and C_{5+} (stable gasoline) components. Therefore, C_2 and C_3 component concentrations are considered indicators of the separation abilities of the absorption and reabsorption towers. Similar to this, the concentrations of C_{3-4} and C_{5-6} components can be used to gauge how well the stabilization towers work during separation. Here, Figure 4a,b displays the concentration distributions of the C_2 and C_3 components, as well as the C_{3-4} and C_{5-6} components. Since absorbent naphtha is fed from the absorption tower's top, it is simple to transport some petrol components there. This portion of the petrol carryover must be recovered in the reabsorber using diesel as an absorbent.

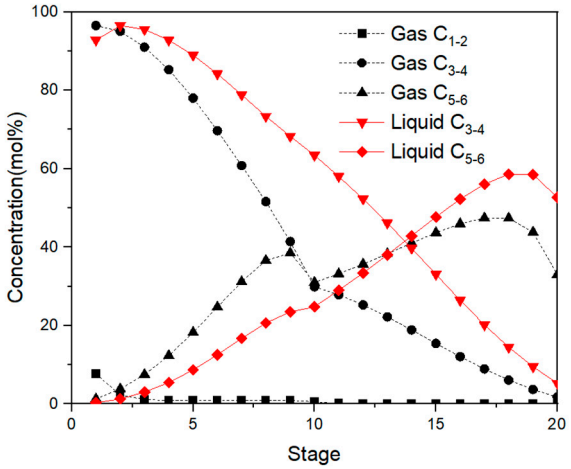


(**a**)

Figure 4. *Cont.*



(**b**)



(**c**)

Figure 4. Concentration distribution curves of key components for (**a**) the absorption tower, (**b**) the reabsorption tower, and (**c**) the stabilization tower in the existing process.

Ethane and ethylene concentrations for the absorption tower are depicted in Figure 4a as steadily increasing from bottom to top, but propane and propylene concentrations are the opposite. The lean dry gas (S9) from the top of the absorption tower will carry part of the absorbent. In order to recover this part of the absorbent, lean absorption oil with light ends of components similar to naphtha is used as a re-absorbent to recover naphtha. It can be seen from Table 2 that the boiling point ranges of naphtha and lean absorption oil overlap, which means that their components are similar. Part of the C_2- components can be dissolved in the absorbent, resulting in a decrease in the C_2- concentration in the early stages of the absorber, as shown in Figure 4a.

The mole fraction of C_3 components in the gas phase on the first stage for the desorption tower is just 0.087%, as illustrated in Figure 4b. As depicted in Figure 4b, the mole fractions of C_2 and lighter components and C_5 and heavier components for the stabilization tower are 2.9% and 0.3%, respectively, and both are within LPG standards.

The Aspen Plus program defaults the reboiler as a theoretical plate, and the last plate can only be written as N-1. The 20th plate in the stabilizer is the reboiler. The concentration of C_{5-6} (gas) decreases in the reboiler of the stabilization tower since it evaporates back to the bottom of the tower, as shown in Figure 4c.

The detailed specification for dry gas, LPG, and stabilized gasoline are given in Table 5.

Table 5. Product Specifications.

Stream	Stream Name	Specifications (Mole Fraction)
Dry gas	S25	C_3 and heavier components $\leq$ 3%
LPG	S24	C_2 and lighter components $\leq$ 3%
	S24	C_5 and heavier components $\leq$ 1.5%
Stabilized Gasoline	S21	C_3 and C_4 components $\leq$ 1%

3.3. System Optimization Parameters

The compression of rich gas depends on the expansion of a medium-pressure steam turbine to do its work. The larger the compression ratio, the more steam will be consumed for doing work, which determines the operating pressure of the absorption tower and constitutes the main energy-consuming part of the GCS. In addition to operating pressure, the absorption effect of the absorber is also closely related to the temperature and flow rate of the absorbent and supplementary absorbent in the absorption tower. The higher the absorbent's circulation volume, the less pressure the rich gas needs to be compressed to have the same absorption effect. In this instance, while the compressor requires less steam, the pump consumes more power. In contrast, the rich gas needs to be compressed to a higher pressure for the same absorption effect since the absorbent's circulation volume is smaller. In this instance, the compressor consumes more energy than the pump. The absorption effect influences the separation energy consumption of other towers in a direct manner. This study focuses on the optimization of the GCS and ASS's operating parameters.

3.3.1. Objective Function

The rich gas compressor is powered by medium-pressure steam in the process flow. Electricity is utilized to power the pumps that deliver crude gasoline and stabilized gasoline, respectively, as an absorbent and supplementary absorbent to the absorption tower. Therefore, it is important to take into account both medium-pressure steam and electricity simultaneously. Since this study focuses on the operational optimization of the existing process, our primary goal is to reduce the system's operational costs.

$$\min C = C_s \times F_s + C_e \times P_e \tag{1}$$

where C_s and C_e represent the price of medium-pressure steam, electricity, which are \$50.15/t and \$0.13/kWh, respectively [19]; F_s: medium-pressure steam usage, t/h; P_e: pump's power consumption, kWh/h.

3.3.2. Manipulate Variables

Absorption, reabsorption, desorption, and stabilization towers are interconnected and influence one another within the FCC ASS. In addition to modifying the output pressure of the compressor in GCS, it is necessary to adjust the parameters of each tower to achieve optimal operation in ASS. Manipulated variables include flowrate of the absorbent (F_{abs}), flowrate of the Supplementary absorbent (F_{sup}), medium-pressure steam consumption (F_s), reflux ratio and reboiler load of stabilizer (RR_{sta} and $Q_{sta-reb}$), inlet temperature of absorbent (T_{abs}) and Desorber Reboiler Load($Q_{des-reb}$).

$$L_1 < F_{abs} < U_1 \tag{2}$$

$$L_2 < F_{sup} < U_2 \tag{3}$$

$$L_3 < F_s < U_3 \tag{4}$$

$$L_4 < RR_{sta} < U_4 \tag{5}$$

$$L_5 < Q_{sta-reb} < U_5 \quad (6)$$

$$L_6 < T_{abs} < U_6 \quad (7)$$

$$L_7 < Q_{des-reb} < U_7 \quad (8)$$

3.3.3. Constraint Conditions

To ensure that the products (dry gas, liquefied petroleum gas, and stabilized gasoline) obtained by the simulation of the absorption stabilization system meet the process indicators while simultaneously optimizing the compressor outlet pressure, absorbent, and supplementary absorbent dosage, it is necessary to impose constraints to ensure that the optimization also satisfies the constraints as follows:

$$y_{C3+,S25} < 0.03 \quad (9)$$

$$y_{C2-,S24} < 0.03 \quad (10)$$

$$y_{C5+,S24} < 0.015 \quad (11)$$

$$y_{C4-,S24} < 0.01 \quad (12)$$

$$y_{C2-,S14} < 0.007 \quad (13)$$

3.4. Optimization and Analysis

The objective function is defined within the optimization model in Aspen Plus Analysis Tools, minimizing the operational cost of medium-pressure steam and electricity for the system. The upper and lower bounds of manipulated variables are also defined in the optimization block. Flowrate of the absorbent, the flow rate of the Supplementary absorbent, medium-pressure steam consumption, reflux ratio, reboiler load of stabilizer, inlet temperature of absorbent, and Desorber Reboiler Load were considered as decision variables in the optimization. The Constraints are defined within the constraint model in Aspen Plus Analysis Tools, including quality specifications for dry gas, liquefied petroleum gas, and stabilized gasoline. The SQP optimization algorithm is used in Aspen Optimizer. The SQP algorithm is designed to handle both equality and inequality constraints. It incorporates the constraints into the optimization problem, ensuring that the solution satisfies the specified constraints. This makes it useful for problems where constraints on process variables or system limitations need to be considered during optimization.

The Base case is from the FCC Rich Gas Compression System and Absorption-stabilization System in fuel-based refineries. The entire system is simulated using the commercial software environment Aspen Plus V12.0, and it is optimized using the optimization module of model analysis software. The stream parameters of the Steam Turbine and rich gas compressor in GCS are illustrated in Table 6.

Table 6. Stream parameters of Steam Turbine and rich gas compressor in GCS.

Description	Data
Rich gases rate-compressor inlet [t/h]	85.1
Rich gas inlet temperature [°C]	33
Rich gas inlet pressure [MPa]	0.34
Rich gas outlet temperature [°C]	105
Rich gas outlet pressure [Mpa]	1.26
Turbine inlet steam flowrate [kg/h]	46,180
Turbine inlet steam pressure [Mpa]	3.6
Turbine inlet steam temperature [°C]	331
Turbine outlet steam flowrate [kg/h]	46,180
Turbine outlet steam pressure [Mpa]	1
Turbine outlet steam temperature [°C]	206
Turbine isentropic efficiency	0.75
Turbine mechanical efficiency	0.95

The feed temperature of the absorbent has both positive and negative effects on the total energy consumption of the system. In particular, the low feed temperature of the absorbent helps decrease the concentrations of C_{3+} components, and flow rate of the dry gas, thus maximizing the recovery of propylene and butene. However, a low feed temperature of absorbent increases the content of C_{2+} and flow rate of the feed stream from the gas-liquid separation tank, which inevitably raises the cold load of absorption tower and the heat load of desorption tower to meet the product specifications. On the contrary, the higher feed temperature of the absorbent is harmful to improving the absorbing efficiency of the absorption tower while increasing the energy requirement of the pumps and compressors, as well as the reboiler duty of the desorber and stabilizer. Therefore, we need to appropriately adjust the feed temperature of the absorbent to determine the trade-off between product quality and energy requirements. The feed temperature of the absorbent becomes a key design parameter in the new process design and will be investigated later.

Based on the assumption that chilled water is available as a cold utility, the temperature range of the absorbent can be determined by replacing the cooling water with chilled water. By using chilled water instead of cooling water, the absorbent temperature can be maintained within a specific range. For example, let us consider a scenario where the previous cooling water temperature ranged from 25 °C to 35 °C and the absorbent temperature cannot be reduced below 40 °C. By replacing it with chilled water, the absorbent temperature range could be narrowed down to 10 °C to 30 °C. This narrower range can help optimize the absorbent's performance and improve the overall efficiency of the system. Table 7 shows the bounds on these manipulated variables and the results obtained by adjusting the decision variables through the optimization module in Aspen Plus V12.0. The objective function converged at the optimal operational parameters.

Table 7. Comparison between control range and optimal values of operating parameters.

Manipulated Variable	Control Range	Optimal Value
Absorbent flow rate (t/h)	1–200	49.7
Supplementary gasoline flow rate (kmol/h)	1–1000	983
3.5 MPa steam flow rate (t/h)	1–100	38.5
Reflux ratio in stabilizer	0.5–3.5	2.36
Absorbent inlet temperature (°C)	10–30	16.56
Reboiler duty of desorber (MJ/h)	4184–83,680	11.5
Reboiler duty of stabilizer (MJ/h)	4184–83,680	14.9

The higher the compressor outlet pressure, the smaller the amount of stabilized gasoline required as supplemental absorbent to meet the same separation requirements, but at a higher total utility cost. This is because compressors work far less efficiently than pumps and therefore consume more energy.

As stated previously, the utility cost is based on the minimum operating cost of the steam turbine and pump as the objective function, which is calculated by manipulating the decision variables using the optimization module. The operating costs for the base case and after optimization are compared in Table 8.

Table 8. Comparison of utility for the base case and after optimization.

Utility	Base Case	After Optimization
Medium pressure steam consumption, t/h	39.538	38.578
Medium pressure steam cost, $/h	1982.831	1934.687
Power consumption of crude gasoline pump, KW	4.746	4.886
Electricity cost of crude gasoline pump, $/h	0.617	0.635
Power consumption of supplementary gasoline pump, KW	17.068	17.710
Electricity Cost of supplementary gasoline pump, $/h	2.219	2.302
Total Operation Cost, $/h	1985.667	1937.624

According to Table 8, the operating cost prior to optimization was $1985.667/h, whereas it was $1937.624/h after optimization. After calculation, the total savings are $48.043/h, and the annual cost savings are $413,1698 (Based on the annual operation hour of 8600 h). Under optimal conditions of operation, a refinery can save 2.42% of utility expenses when compared to the base scenario of a 725 kt/a rich gas FCC unit.

4. Results and Discussion

Since the absorption tower is the core equipment connecting the rich gas compression system and the system stabilization system, it is necessary to optimize the decision variables, such as the amount of absorbent (crude gasoline) and supplementary absorbent (stabilized gasoline) to the absorption tower. The pressure of the absorption tower is determined by the rich gas compressor, so it is necessary to optimize the outlet pressure of the rich gas compressor as well. To achieve the expected goal of minimizing the operating costs of steam turbines and pumps as the objective function, the compressor outlet pressure was reduced from 1300 kPa (prior to optimization) to 1260 kPa (after optimization). Under optimal operation, a refinery can save 2.42% of utility expenses, when compared to the base scenario of a 725 kt/a rich gas FCC unit.

To compensate for the effect of pressure reduction, the circulation volume of absorbent and supplementary absorbent is increased, thereby enhancing the absorption effect of light components C_{3+} in the absorption tower as a whole. The C_{2-} light components are supposed to separate from the top of the absorption tower, thereby reducing the amount of C_{2-} light components fed to the stabilization tower. However, the absorption effect of the absorption tower should not be too high; otherwise, the operating cost of the desorption tower will increase.

It is important to note that the absorbent's inlet temperature is 16.56 °C when operating expenses are at their lowest. Since the temperature of the absorbent is limited by the temperature of the cooling water supply, it is difficult to achieve the best absorption effect of the absorption tower, and future research will employ the lithium bromide absorption refrigeration system to recover the heat of the high-temperature stable gasoline in the stabilization system to supply refrigerant water, replacing the traditional circulating cooling water system as the cold source of the absorbent. This strategy can be considered to cool the absorbent temperature of the absorption tower to a lower temperature, thereby improving the absorption effect and the economic efficiency of the whole system.

5. Conclusions

This study concentrates on the impact of the rich gas compressor's outlet pressure on the absorption stabilization system to reduce the system's operating expenses. Using Aspen Plus V12.0, a rich gas compression and absorption stabilization system was simulated and optimized. Two conclusions can be drawn from this study. First, by increasing the circulation volume of the absorbent, it is possible to reduce the outlet pressure of the rich gas compressor and the utility cost of the system, assuming the product separation accuracy requirements are met. Secondly, the conventional absorbent temperature is 30 °C. If chilled water is used to cool the absorbent, the temperature of the absorbent can be lowered, which helps to improve the absorption effect of the absorption tower. The use of chilled water systems has advantages over circulating water systems, which can cool the process stream to a lower temperature. The lithium bromide absorption refrigeration cycle system is assumed to be used to produce chilled water. The control range of absorbent inlet temperature is set to 10–30 °C, with chilled water available as cold utility. The implementation of optimized operations has led to a noteworthy reduction of 2.4% in medium-pressure steam consumption compared to the initial conditions. This reduction has resulted in a substantial enhancement in the overall cost-effectiveness of operations. The results show that optimizing compressor outlet pressure, temperature, and dosage of absorbent simultaneously can effectively improve project economics and energy-use performance.

Author Contributions: Conceptualization, J.S.; methodology, J.S. and L.W.; software, Z.Y.; validation, H.Y., J.S. and R.Z.; formal analysis, J.S.; investigation, H.Y.; resources, L.W.; data curation, R.Z.; writing—original draft preparation, J.S.; writing—review and editing, H.Y.; visualization, Z.Y.; supervision, L.J.; project administration, S.H.; All authors have read and agreed to the published version of the manuscript.

Funding: This research was funded by talent introduction program of Guangdong University of Petrochemical Technology (2020rc009) and Guangdong Provincial Natural Science Foundation Project (2023A1515012341).

Data Availability Statement: Not applicable.

Conflicts of Interest: The authors declare no conflict of interest.

Nomenclature

ASS	Absorption-stabilization System
FCC	Fluid catalytic cracking
FCCU	Fluid catalytic cracking unit
GASP	Gasoline Absorption–Stabilization Process
GCS	Gas compression system
HPS	High pressure separator
LPG	Liquefied petroleum gas
MIP	Maximizing iso-paraffins
ORC	Organic rankine cycle
RVP	Reid Vapor Pressure
TBP	True boiling point
Streams	
S1	Compressor 1st stage inlet rich gas
S2	Compressor 1st stage outlet rich gas
S3	Air cooler inlet stream
S4	Air cooler outlet stream
S5	Gas separated from gas-liquid separation tank
S6	liquid separated from gas-liquid separation tank
S7	Crude naphtha as absorbent
S8	Crude naphtha after cooler

S9	Lean dry gas from top of absorber
S10	Absorber bottom oil before pump P2
S11	Condensate oil
S12	Desorbed gas from the desorber
S13	Absorber bottom oil after pump P2
S14	De-ethanized gasoline
S15	Desorber bottom oil before pump P3
S16	Desorber bottom oil after pump P3
S17	LPG from top of stabilizer
S19	Stabilized gasoline from bottom of stabilizer
S20	Stabilized gasoline before pump P4
S21	Stabilized gasoline after pump P4
S22	Stabilized gasoline as supplementary absorbent
S23	LPG as reflux stream
S24	Liquefied petroleum gas
S25	Dry gas
S26	Lean absorption oil to the reabsorber
S27	Rich absorption oil from the bottom of reabsorber
S28	Pumparound stream to intermediate cooler
Equipment	
D1–D3	Gas-liquid separation tank
E1	Air cooler
E10	Interstage cooler
E2–E6	Cooling water cooler
E7–E8	Reboiler
E9	Heat exchanger
P1–P7	Pumps
T1	Absorber
T2	Desorber
T3	Reabsorber
T4	Stabilizer

Appendix A

Table A1. Data of streams on the rich gas compression system and absorption stabilization system.

Variable	Streams												
	S3	**S5**	**S6**	**S9**	**S10**	**S12**	**S14**	**S7**	**S21**	**S24**	**S25**	**S26**	**S27**
T(C)	48.02	33.00	33.00	43.00	49.55	44.30	120.49	30.00	194.37	46.16	29.38	10.00	48.82
P(Mpa)	1.26	1.26	1.26	1.24	1.25	1.5	1.53	1.2	1.23	1.2	1.13	1.2	1.143
Mole Flow (kmol/h)	4321.17	1380.68	2940.49	924.65	1925.18	327.00	2613.50	490.04	1669.33	944.17	884.66	79.97	119.96
Mass Flow(kg/h)	272,718.32	40,001.26	232,717.06	21,894.53	177,242.21	11,120.47	221,596.58	56,654.22	174,725.61	46,871.13	19,226.84	17,448.96	20,116.65
Composition (mol/mol)													
CH_4	0.0668	0.1827	0.0124	0.2488	0.0115	0.1116	0.0000	0.0000	0.0000	0.0000	0.2581	0.0000	0.0142
C_2H_6	0.0616	0.1120	0.0379	0.1032	0.0307	0.2591	0.0103	0.0000	0.0000	0.0284	0.1044	0.0000	0.0260
C_3H_8	0.0613	0.0586	0.0625	0.0006	0.0418	0.0662	0.0620	0.0000	0.0000	0.1717	0.0005	0.0000	0.0004
C_4H_{10}-2	0.0540	0.0267	0.0669	0.0008	0.0197	0.0295	0.0715	0.0000	0.0019	0.1946	0.0006	0.0000	0.0013
C_4H_{10}-1	0.0209	0.0080	0.0270	0.0013	0.0073	0.0090	0.0292	0.0000	0.0043	0.0734	0.0010	0.0000	0.0029
C_5H_{12}-2	0.0563	0.0101	0.0779	0.0184	0.0639	0.0118	0.0862	0.0000	0.1288	0.0110	0.0071	0.0000	0.0893
C_5H_{12}-1	0.0076	0.0011	0.0107	0.0020	0.0091	0.0013	0.0119	0.0000	0.0184	0.0003	0.0004	0.0000	0.0124
C_6H_{14}-1	0.0589	0.0028	0.0852	0.0059	0.0752	0.0037	0.0954	0.0000	0.1494	0.0000	0.0000	0.0000	0.0457
C_2H_4	0.0517	0.1082	0.0252	0.1176	0.0212	0.2261	0.0000	0.0000	0.0000	0.0001	0.1200	0.0000	0.0210
C_3H_6-2	0.1194	0.1251	0.1167	0.0074	0.0862	0.1435	0.1134	0.0000	0.0000	0.3138	0.0071	0.0000	0.0048
C_4H_8-1	0.0205	0.0090	0.0259	0.0005	0.0070	0.0100	0.0279	0.0000	0.0015	0.0744	0.0004	0.0000	0.0010
C_4H_8-2	0.0140	0.0048	0.0183	0.0013	0.0052	0.0054	0.0199	0.0000	0.0047	0.0468	0.0009	0.0000	0.0032
C_4H_8-3	0.0106	0.0039	0.0138	0.0006	0.0036	0.0044	0.0150	0.0000	0.0021	0.0377	0.0005	0.0000	0.0014
C_4H_8-5	0.0124	0.0055	0.0156	0.0003	0.0042	0.0061	0.0167	0.0000	0.0008	0.0449	0.0002	0.0000	0.0005
C_4H_6-4	0.0003	0.0001	0.0004	0.0000	0.0001	0.0001	0.0004	0.0000	0.0000	0.0011	0.0000	0.0000	0.0000
H_2	0.0377	0.1157	0.0011	0.1703	0.0012	0.0100	0.0000	0.0000	0.0000	0.0000	0.1778	0.0000	0.0015
N_2	0.0548	0.1631	0.0040	0.2352	0.0040	0.0359	0.0000	0.0000	0.0000	0.0000	0.2451	0.0000	0.0053
O_2	0.0068	0.0195	0.0008	0.0275	0.0008	0.0075	0.0000	0.0000	0.0000	0.0000	0.0286	0.0000	0.0010
CO	0.0037	0.0110	0.0003	0.0159	0.0003	0.0026	0.0000	0.0000	0.0000	0.0000	0.0166	0.0000	0.0004
CO_2	0.0116	0.0251	0.0052	0.0277	0.0046	0.0470	0.0000	0.0000	0.0000	0.0000	0.0283	0.0000	0.0049
PC32C	0.0224	0.0035	0.0313	0.0071	0.0495	0.0041	0.0346	0.0917	0.0533	0.0017	0.0022	0.0000	0.0388
PC59C	0.0129	0.0009	0.0186	0.0019	0.0289	0.0011	0.0208	0.0494	0.0325	0.0000	0.0000	0.0000	0.0144
PC73C	0.0164	0.0007	0.0238	0.0015	0.0367	0.0009	0.0266	0.0616	0.0417	0.0000	0.0000	0.0000	0.0117
PC87C	0.0280	0.0008	0.0409	0.0016	0.0628	0.0010	0.0458	0.1042	0.0718	0.0000	0.0000	0.0000	0.0126
PC100C	0.0283	0.0005	0.0414	0.0011	0.0635	0.0007	0.0465	0.1046	0.0728	0.0000	0.0000	0.0000	0.0083
PC114C	0.0253	0.0003	0.0371	0.0006	0.0568	0.0004	0.0417	0.0930	0.0653	0.0000	0.0000	0.0000	0.0045
PC128C	0.0256	0.0002	0.0376	0.0004	0.0575	0.0003	0.0423	0.0939	0.0662	0.0000	0.0000	0.0000	0.0028
PC142C	0.0268	0.0001	0.0394	0.0002	0.0602	0.0002	0.0443	0.0980	0.0693	0.0000	0.0000	0.0026	0.0034
PC156C	0.0242	0.0001	0.0355	0.0001	0.0542	0.0001	0.0399	0.0882	0.0625	0.0000	0.0000	0.0215	0.0151
PC170C	0.0228	0.0000	0.0334	0.0001	0.0511	0.0001	0.0376	0.0830	0.0589	0.0000	0.0000	0.0246	0.0168

Table A1. *Cont.*

Variable	Streams												
	S3	S5	S6	S9	S10	S12	S14	S7	S21	S24	S25	S26	S27
PC184C	0.0156	0.0000	0.0228	0.0000	0.0349	0.0000	0.0257	0.0567	0.0402	0.0000	0.0000	0.0339	0.0227
PC198C	0.0111	0.0000	0.0163	0.0000	0.0249	0.0000	0.0183	0.0404	0.0287	0.0000	0.0000	0.0513	0.0342
PC211C	0.0096	0.0000	0.0142	0.0000	0.0216	0.0000	0.0159	0.0351	0.0249	0.0000	0.0000	0.0649	0.0433
PC226C	0.0000	0.0000	0.0000	0.0000	0.0000	0.0000	0.0000	0.0000	0.0000	0.0000	0.0000	0.1008	0.0672
PC239C	0.0000	0.0000	0.0000	0.0000	0.0000	0.0000	0.0000	0.0000	0.0000	0.0000	0.0000	0.0979	0.0653
PC253C	0.0000	0.0000	0.0000	0.0000	0.0000	0.0000	0.0000	0.0000	0.0000	0.0000	0.0000	0.0899	0.0599
PC267C	0.0000	0.0000	0.0000	0.0000	0.0000	0.0000	0.0000	0.0000	0.0000	0.0000	0.0000	0.0827	0.0551
PC281C	0.0000	0.0000	0.0000	0.0000	0.0000	0.0000	0.0000	0.0000	0.0000	0.0000	0.0000	0.0696	0.0464
PC295C	0.0000	0.0000	0.0000	0.0000	0.0000	0.0000	0.0000	0.0000	0.0000	0.0000	0.0000	0.0629	0.0419
PC309C	0.0000	0.0000	0.0000	0.0000	0.0000	0.0000	0.0000	0.0000	0.0000	0.0000	0.0000	0.0626	0.0417
PC322C	0.0000	0.0000	0.0000	0.0000	0.0000	0.0000	0.0000	0.0000	0.0000	0.0000	0.0000	0.0612	0.0408
PC337C	0.0000	0.0000	0.0000	0.0000	0.0000	0.0000	0.0000	0.0000	0.0000	0.0000	0.0000	0.0632	0.0421
PC351C	0.0000	0.0000	0.0000	0.0000	0.0000	0.0000	0.0000	0.0000	0.0000	0.0000	0.0000	0.0857	0.0571
PC359C	0.0000	0.0000	0.0000	0.0000	0.0000	0.0000	0.0000	0.0000	0.0000	0.0000	0.0000	0.0247	0.0164

References

1. Liu, L.L.; Sun, J.S.; Mei, L.; Wang, Y.H. Design and optimization FCCU absorption-stabilization system through process simulation. *Adv. Mat. Res.* **2012**, *391*, 1400–1405. [CrossRef]
2. Chen, Q.; Yin, Q.; Hua, B. An exergoeconomic approach for retrofit of fractionating systems. *Energy* **2002**, *27*, 65–75. [CrossRef]
3. Sadeghbeigi, R. *Fluid Catalytic Cracking Handbook: An Expert Guide to the Practical Operation, Design, and Optimization of FCC Units*; Butterworth-Heinemann: Oxford, UK, 2020; ISBN 978-0-12-812663-9.
4. Stratiev, D.S.; Shishkova, I.K.; Dobrev, D.S. Fluid catalytic cracking feed hydrotreatment and its severity impact on product yields and quality. *Fuel Process. Technol.* **2012**, *94*, 16–25. [CrossRef]
5. Arbel, A.; Huang, Z.; Rinard, I.H.; Shinnar, R.; Sapre, A.V. Dynamic and control of fluidized catalytic crackers. 1. Modeling of the current generation of FCC's. *Ind. Eng. Chem. Res.* **1995**, *34*, 1228–1243. [CrossRef]
6. Souza, J.A.; Vargas, J.V.C.; Ordonez, J.C.; Martignoni, W.P.; von Meien, O. Thermodynamic optimization of fluidized catalytic cracking (FCC) units. *Int. J. Heat Mass Transf.* **2011**, *54*, 1187–1197. [CrossRef]
7. Li, Z. Operation Optimization of 800 kt/y FCCU Absorption Stabilization System. *Green Pet. Petrochem.* **2018**, *3*, 15–19.
8. Chen, J.Y.; Pan, M.; He, C.; Zhang, B.J.; Chen, Q.L. New Gasoline Absorption–Stabilization Process for Separation Intensification and Flowsheet Simplification in Refineries. *Ind. Eng. Chem. Res.* **2018**, *57*, 14707–14717. [CrossRef]
9. Pan, Q.; Lu, E.; Li, J. Rigorous Dynamic Simulation and Optimization for FCCU Absorption-Stabilization System. *Comput. Aided Chem. Eng.* **2005**, *20*, 499–504.
10. Liu, X.; He, C.; He, C.; Chen, J.; Zhang, B.; Chen, Q. A new retrofit approach to the absorption-stabilization process for improving energy efficiency in refineries. *Energy* **2017**, *118*, 1131–1145. [CrossRef]
11. Zhang, Y.; Li, Z.; Wang, Z.; Jin, Q. Optimization Study on Increasing Yield and Capacity of Fluid Catalytic Cracking (FCC) Units. *Processes* **2021**, *9*, 1497. [CrossRef]
12. Liu, Y.A.; Chang, A.-F.; Pashikanti, K. *Petroleum Refinery Process Modeling: Integrated Optimization Tools and Applications*; Wiley-VCH: Weinheim, Germany, 2018; ISBN 978-3-527-34423-9.
13. Sui, H.; Wu, J.; He, L.; Li, X. Conversion of low-grade heat from FCC absorption-stabilization system to electricity by organic Rankine cycles: Simulation and optimization. *J. Eng. Thermophys.* **2017**, *26*, 216–233. [CrossRef]
14. Yang, L.; Dan-Lin, Z.; Guang-Hui, W.; Qing-Lin, C. Simulation analysis for energy saving process of absorption and stabilization system of intensified absorption process. *Pet. Process. Petrochem.* **2015**, *46*, 83.
15. Pinheiro, C.I.; Fernandes, J.L.; Domingues, L.; Chambel, A.J.; Graça, I.; Oliveira, N.M.; Cerqueira, H.S.; Ribeiro, F.R. Fluid catalytic cracking (FCC) process modeling, simulation, and control. *Ind. Eng. Chem. Res.* **2012**, *51*, 1–29. [CrossRef]
16. He, G.; Zhou, C.; Luo, T.; Zhou, L.; Dai, Y.; Dang, Y.; Ji, X. Online optimization of Fluid Catalytic Cracking process via a Hybrid model based on Simplified structure-Oriented Lumping and case-based reasoning. *Ind. Eng. Chem. Res.* **2020**, *60*, 412–424. [CrossRef]
17. Chen, J.; Xu, Y. *Catalytic Cracking Technology and Engineering*; Sinopec Press: Beijing, China, 2015.
18. Wasylkiewicz, S.K.; Kobylka, L.C.; Castillo, F.J. Synthesis and design of heterogeneous separation systems with recycle streams. *Chem. Eng. J.* **2003**, *92*, 201–208. [CrossRef]
19. Average Energy Prices for the United States, Regions, Census Divisions, and Selected Metropolitan Areas. U.S. Bureau of Labor Statistics. Available online: https://www.bls.gov/regions/midwest/data/averageenergyprices_selectedareas_table.htm (accessed on 10 July 2023).

Disclaimer/Publisher's Note: The statements, opinions and data contained in all publications are solely those of the individual author(s) and contributor(s) and not of MDPI and/or the editor(s). MDPI and/or the editor(s) disclaim responsibility for any injury to people or property resulting from any ideas, methods, instructions or products referred to in the content.